STRUCTURAL CHEMISTRY

ISSN 2053-2296

Pyridine-4-thiol as halogen-bond (HaB) acceptor: influence of the noncovalent interaction in its reactivity

Marta E. G. Mosquera,[a]* Silvia Dortez,[b] Francisco Fernández-Palacio[a] and Pilar Gómez-Sal[a]

[a]Department of Organic and Inorganic Chemistry, Institute of Chemical Research 'Andrés M. del Río' (IQAR), Universidad de Alcalá, Campus Universitario, 28871 Alcalá de Henares, Madrid, Spain, and [b]Department of Analytical Chemistry, Physical Chemistry and Chemical Engineering, Institute of Chemical Research 'Andrés M. del Río' (IQAR), Universidad de Alcalá, Campus Universitario, 28871 Alcalá de Henares, Madrid, Spain. *Correspondence e-mail: martaeg.mosquera@uah.es

Received 1 December 2022
Accepted 3 March 2023

Edited by A. Peuronen, University of Sheffield, United Kingdom

Keywords: halogen bond; HaB; pyridine-4-thiol; C—Cl bond activation; crystal structure; chalcogen bond.

CCDC references: 2222766; 2222767

Supporting information: this article has supporting information at journals.iucr.org/c

The study of pyridine-4-thiol as a halogen-bond (HaB) acceptor has allowed the isolation of its cocrystal with the HaB donor IC_6F_4I, namely, 1,2,4,5-tetrafluoro-3,6-diiodobenzene bis(pyridin-1-ium-4-ylsulfanide), $C_6F_4I_2{\cdot}2C_5H_5NS$ (**1**), where the S atom is the HaB acceptor, while the pyridine position is blocked by the proton. Furthermore, the S atom acts a dual acceptor and also establishes an interaction with the pyridinium proton from an adjacent molecule. The presence of these interactions in **1** contributes to the stabilization of the zwitterionic form. This pre-organization seems to have an influence on the reactivity of the compound since when left in dichloromethane solution, an unusual activation of the C—Cl bond is observed that leads to the formation of the bis[(pyridin-1-ium-4-yl)sulfanyl]methane dication, while the Cl atoms are still present as chloride counter-ions, *i.e.* 4,4′-[methanediyldi(sulfanediyl)]dipyridinium dichloride, $C_{11}H_{12}N_2S_2^{2+}{\cdot}2Cl^-$ (**2**). In the crystal structure of **2** it is observed that the S atom is now acting as the donor part of a chalcogenide bond with the chloride anions.

1. Introduction

Halogen bonding (HaB) is a noncovalent interaction that has attracted increasing attention during the last few decades, due to its role in crystal engineering, molecular recognition processes, as a structure-directing tool and for the modulation of some physical properties (Politzer *et al.*, 2007; Brammer *et al.*, 2001; Aakeröy *et al.*, 2013; Cavallo *et al.*, 2016). Also, its influence in reactivity and catalysis is increasingly acknowledged (Bulfield & Huber, 2016; Bamberger *et al.*, 2019; Jónsson *et al.*, 2022).

In our group, we have explored this interaction in metallic complexes, both for main group and transition metals, and have observed the influence of HaB in the structural arrangement and reactivity (Dortéz *et al.*, 2020; Mosquera *et al.*, 2016, 2017; Vidal *et al.*, 2013). In this work, we are interested in exploring pyridine-4-thiol as a HaB acceptor since there are two possible sites able to act as such, namely, the pyridine group and the S atom. Pyridines are one of the most popular types of HaB acceptor, a search in the Cambridge Structural Database (CSD; Version 5.42, with updates to September 2021; Groom *et al.*, 2016) for HaB interactions with C—*X* (*X* = Br or I) gives over 1000 hits. On the other hand, sulfur has two available lone pairs and can be a potent HaB acceptor since it can interact with more than one HaB donor, which can lead to interesting topologies. However, it has been less studied, although in a search in the CSD, there is a

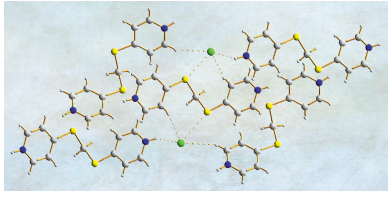

Table 1
Experimental details.

Experiments were carried out at 200 K with Mo $K\alpha$ radiation using a Nonius KappaCCD diffractometer. H atoms were treated by a mixture of independent and constrained refinement.

	1	**2**
Crystal data		
Chemical formula	$C_6F_4I_2{\cdot}2C_5H_5NS$	$C_{11}H_{12}N_2S_2^{2+}{\cdot}2Cl^-$
M_r	624.18	307.25
Crystal system, space group	Monoclinic, $P2_1/c$	Orthorhombic, $F2dd$
a, b, c (Å)	16.288 (8), 5.790 (4), 10.546 (9)	8.0815 (4), 17.2161 (5), 18.9254 (12)
α, β, γ (°)	90, 104.77 (3), 90	90, 90, 90
V (Å^3)	961.7 (12)	2633.1 (2)
Z	2	8
μ (mm^{-1})	3.53	0.79
Crystal size (mm)	0.21 × 0.18 × 0.15	0.4 × 0.3 × 0.25
Data collection		
Absorption correction	Multi-scan (Blessing, 1995)	–
T_{min}, T_{max}	0.371, 0.426	–
No. of measured, independent and observed $[I > 2\sigma(I)]$ reflections	3983, 2181, 1458	4579, 1386, 1177
R_{int}	0.040	0.069
$(\sin\theta/\lambda)_{max}$ (Å^{-1})	0.649	0.650
Refinement		
$R[F^2 > 2\sigma(F^2)]$, $wR(F^2)$, S	0.032, 0.069, 0.93	0.041, 0.101, 1.10
No. of reflections	2181	1386
No. of parameters	122	84
No. of restraints	0	1
$\Delta\rho_{max}$, $\Delta\rho_{min}$ (e Å^{-3})	0.99, −1.09	0.35, −0.30
Absolute structure	–	Flack x determined using 445 quotients $[(I^+) - (I^-)]/[(I^+) + (I^-)]$ (Parsons *et al.*, 2013)
Absolute structure parameter	–	−0.01 (11)

Computer programs: *COLLECT* (Nonius, 2004), *DIRAX/LSQ* (Duisenberg *et al.*, 2003), *EVALCCD* (Duisenberg *et al.*, 2003), *SHELXT2018* (Sheldrick, 2015*a*), *SHELXS2013* (Sheldrick, 2008), *SHELXL2014* and *SHELXL2016* (Sheldrick, 2015*b*), *ORTEP-3 for Windows* (Farrugia, 2012) and *WinGX* (Farrugia, 2012).

significant number of structures that display S atoms as a HaB acceptor; a search for C—$X\cdots$S (X = Br or I) interactions in the angle range 160–180° gave 715 hits.

We have explored the interaction of pyridine-4-thiol with the iconic IC_6F_4I molecule as HaB donor. Interestingly, for this molecule, it is not the pyridine group but the S atom that acts as the HaB acceptor, which is surprising since in the related compound Py–S–Py, it is the pyridine group that acts as the HaB acceptor (Arman *et al.*, 2010). Furthermore, the presence of C—S$\cdots$I interactions in this cocrystal favours the stabilization of the zwitterionic form for pyridine-4-thiol (namely, pyridin-1-ium-4-ylsulfanide), which has important implications in the reactivity of the molecule, and in fact an unusual C—Cl activation of the dichloromethane solvent is observed to give the bis[(pyridin-1-ium-4-yl)sulfanyl]methane dication.

The structures of 1,2,4,5-tetrafluoro-3,6-diiodobenzene bis(pyridin-1-ium-4-ylsulfanide), **1**, and 4,4′-[methanediyldi(sulfanediyl)]dipyridinium dichloride, **2**, are reported.

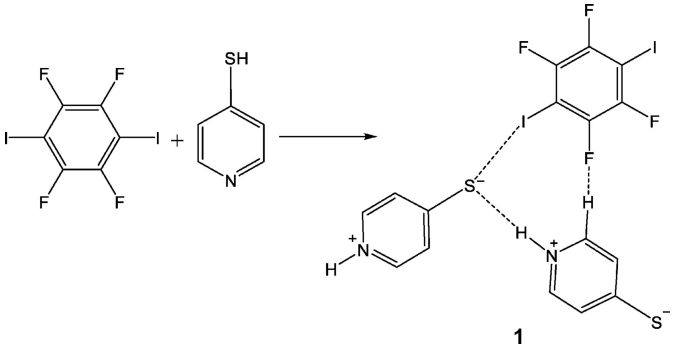

Figure 1
The synthetic scheme for the preparation of cocrystal **1**.

2. Experimental

2.1. General considerations

All manipulations were carried out under an inert atmosphere of argon using standard Schlenk techniques. All solvents were dried prior to use following standard methods. All reagents were commercially obtained and were used without further purification.

2.2. Synthesis and crystallization

2.2.1. Synthesis of cocrystal 1. Pyridine-4-thiol (14 mg, 0.126 mmol) and 1,2,4,5-tetrafluoro-3,6-diiodobenzene (50 mg, 0.126 mmol) were placed in a Schlenk flask. To this mixture, CH_2Cl_2 (25 ml) and tetrahydrofuran (12 ml) were added. In order to completely dissolve the solid, a brief reflux with a heat gun was performed. The solution was filtered and left to evaporate slowly. After three weeks, yellow crystals were isolated (yield: 63%, 40 mg).

2.2.2. Synthesis of (HPy–CH_2–PyH)Cl_2 (2). To pyridine-4-thiol (50 mg, 0.45 mmol) in a Schlenk flask was added CH_2Cl_2 (10 ml). To this suspension, $C_6F_4I_2$ (180 mg, 0.45 mmol) was added and, to dissolve the mixture completely, tetrahydrofuran (10 ml) were added. The solution was left to stir for 48 h. A clear solution was formed, to which a layer of hexane (16 ml) was added. After the solution had diffused into the hexane, brown crystals of **2** of good enough quality for analysis by X-ray diffraction were isolated (yield: 32%, 22 mg).

2.3. Refinement

Crystal data, data collection and structure refinement details are summarized in Table 1. H atoms were placed geometrically and left riding on their parent atoms, except for the H atoms bonded to N1 in cocrystal **1**, and C10 and N1 in salt **2**, which were found in a Fourier map.

3. Results and discussion

In order to achieve the crystallization of pyridine-4-thiol and IC_6F_4I, both compounds were dissolved in a mixture of CH_2Cl_2 and tetrahydrofuran under argon. The suspension was heated briefly to obtain a clear solution (Fig. 2). From this, orange crystals were isolated after three weeks by slow evaporation and the structure was determined by X-ray diffraction analysis.

Table 2
Selected interatomic distances (Å) and angles (°) for **1** and **2**.

1		**2**	
I1···S2	3.158 (7)	C10—S1	1.800 (4)
C1—S1	1.708 (5)	C1—N1	1.344 (7)
C6—I1	2.107 (4)	C5—S1	1.743 (5)
F2···H3	2.583 (7)		
C4—N1—C3	121.7 (4)	S1—C10—S1^{i}	116.3 (4)
F1—C7—C6	120.1 (4)	N1—C1—C6	120.4 (5)
C7—C6—I1	121.0 (3)	C5—S1—C10	104.89 (19)

Symmetry code: (i) $x, -y+\frac{5}{2}, -z+\frac{3}{2}$.

As shown in Fig. 2, a cocrystal has been formed incorporating two molecules of pyridine-4-thiol and one of IC_6F_4I. This compound crystallized in the monoclinic space group $P2_1/c$. In this case, it is the S atom that acts as the HaB acceptor, which stabilizes the zwitterionic form of pyridine-4-thiol and, at the same time, the pyridine group is blocked by the proton. It should be noted that pyridine-4-thiol has been used frequently as a ligand for *d*- and *f*-block metals, and in those cases most often the zwitterionic form is the one present (CSD; Groom *et al.*, 2016).

For the HaB established between the pyridine-4-thiol and the perfluorinated unit, the S···I distance is particularly short [3.158 (7) Å and C—I···S = 175.74 (5)°; Table 2]; considering that the van der Waals radius sum is 3.78 Å (Bondi, 1964), this interaction implies a significant reduction of 16.4%. This short distance has also been observed in other compounds and, in all cases, the S atom has a negative charge, as in ours, as

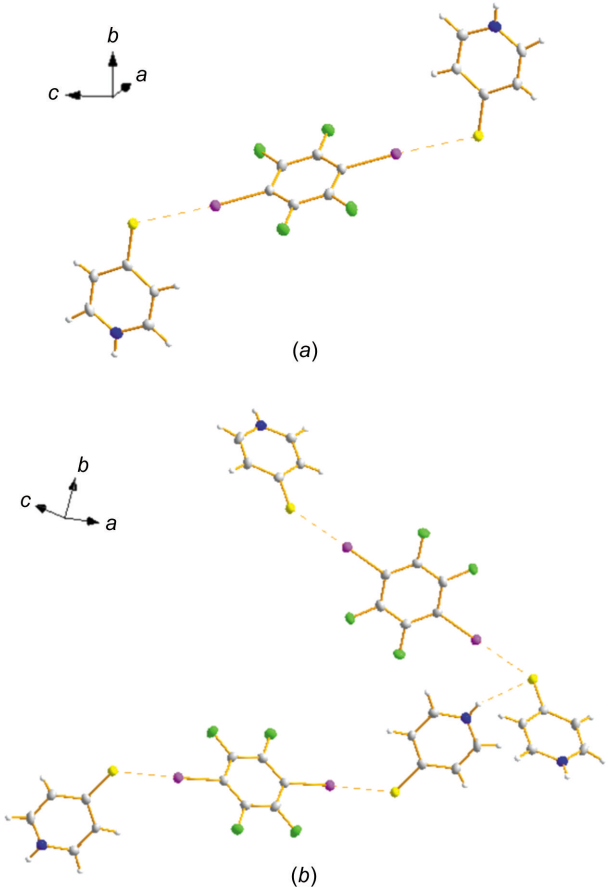

Figure 2
Displacement ellipsoid plot (30% probability) of **1**, showing (*a*) the C—I···S halogen bonding and (*b*) a view of the molecular packing *via* halogen and hydrogen bonding (dashed lines).

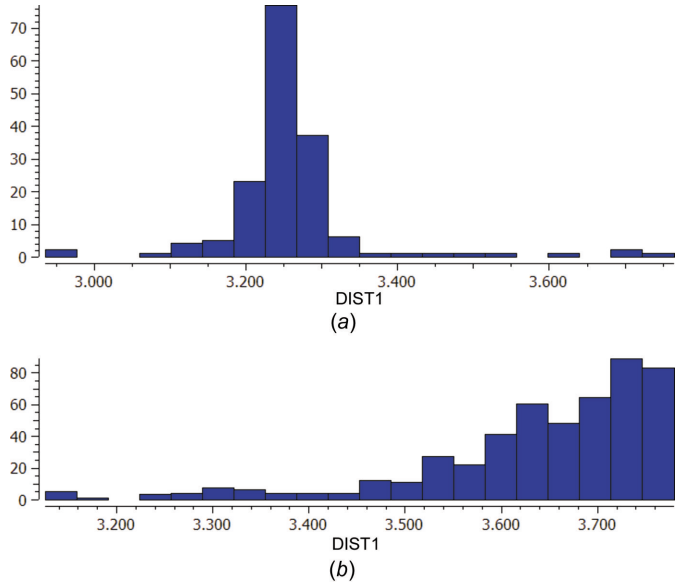

Figure 3
Histograms of the S···I distances for the S···I—C interaction for (*a*) an S atom with a −1 charge (149 hits) and (*b*) an S atom with no charge (339 hits). In salt **2**, the S···I distance is 3.158 (7) Å.

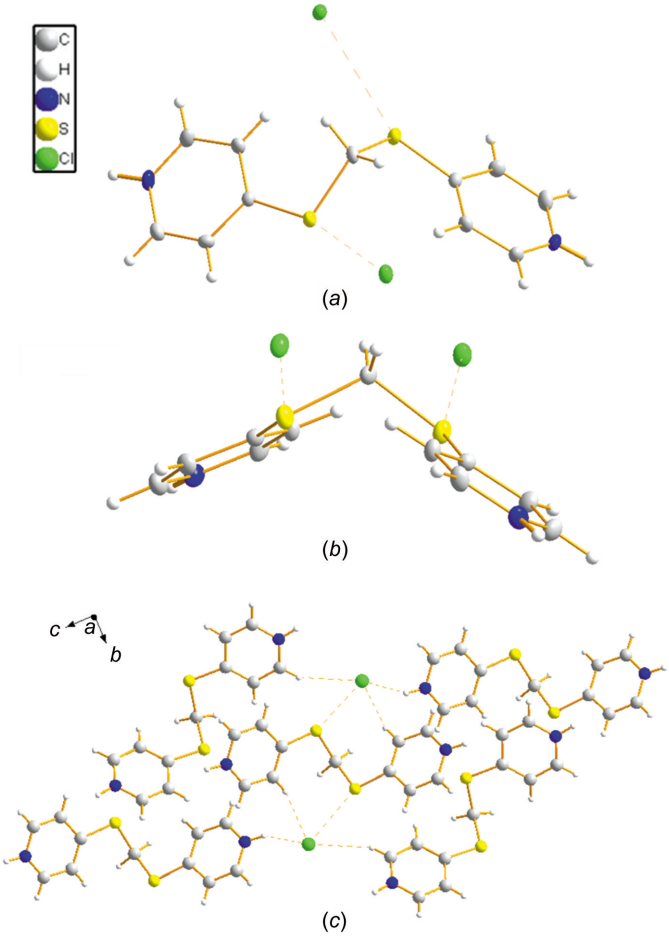

Figure 4
Displacement ellipsoid plot (30% probability) of **2**, showing (*a*) a view along the *bc* plane, (*b*) a view along the *a* direction and (*c*) a view of the packing directed by hydrogen and chalcogen bonds.

evidenced by a search in the CSD. As shown in Fig. 3(*b*), when the S atom is neutral, the majority of the interactions appear at S···I distances over 3.5 Å. For shorter distances [Fig. 3(*a*)], the majority of the examples imply the thyocyanate anion, SCN^- (Zuluaga *et al.*, 2020; Postnikov *et al.*, 2015; Bozopoulos & Rentzeperis, 1986; Hirschberg *et al.*, 2014).

Sulfur can form bifurcated interactions and in this case behaves as such; on one side it interacts with the I atom and on the other side with the pyridinium N—H proton. This behaviour as a dual acceptor for both a halogen and a H atom has been observed previously; however, there are not many examples (Ding *et al.*, 2020).

The perfluorinated unit, *p*-$C_6F_4I_2$, interacts from both sides to give discrete units formed by the interaction of two molecules of pyridine-4-thiol. These units are linked *via* weaker N—H···I and C—H···F interactions to give layers. As mentioned before, for the related Py–S–Py derivative, the interaction is established between the pyridine group and the I atom to give an $N_{Py}\cdots I—C$ contact ($N_{Py}\cdots I$ = 2.838 Å and $N_{Py}\cdots I—C$ = 177.93°) (Arman *et al.*, 2010). Hence, the preference for one group or the other is not very strong and may even be governed by kinetics and, if there is a competing aceptor, such is in the case of the proton, may direct the choice of the donor. In fact, for the thiocyanate, which can also act as a dual donor, the formation of both HaB interactions with the N or the S atom has also been oberved for the same donors (Soldatova *et al.*, 2020).

When the reaction is performed on a larger scale and left stirring for 48 h, the solution changes colour to brown. It was possible to obtain crystals from this solution by diffusion into a hexane layer. The isolated brown crystals were of good enough quality to be determined by single-crystal X-ray diffraction. Interestingly, a methylene-bridged sulfide resulting from the displacement of both Cl atoms from dichloromethane by two molecules of pyridine-4-thiol, *i.e.* an $[L_2CH_2]^{2+}$ dication, is formed. The displaced Cl atoms are still present as chloride counter-ions of the dication generated. The activation of the C—Cl bond has been observed previously, most often *via* a radical mechanism and less frequently *via* a nucleophilic mechanism. In fact, in our group, we have observed a similar reactivity when a zwitterionic betaine derivative composed of a nucleophilic carbene and a carbodimide (CDI-NHC) is left stirring for a long time in a dichloromethane solution (Sánchez-Roa *et al.*, 2018). As in this case, the activation of the C—Cl bond is promoted by the presence of zwitterionic species. As mentioned before, the zwitterionic form of pyridine-4-thiol is stabilized by the presence of the HaB interaction, which implies a pre-organization that influences the outcome of the reaction. A similar behaviour has been described previously for isocyanates (Soldatova *et al.*, 2020).

Moreover, the evolution of pyridine-4-thiol in solution when it is left stirring in solution at 67 °C for 15 h gives the $[HS–Py–Py]^+$ derivative, as has been reported previously (Ding *et al.*, 2020). In our case, the presence of IC_6F_4I favours the competitive reaction that implies the CH_2Cl_2 activation.

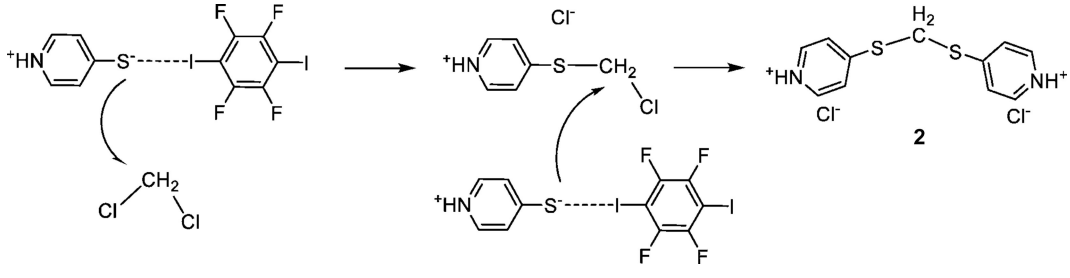

Figure 5
The proposed mechanism for the formation of salt **2**.

Compound **2** crystallized in an orthorhombic noncentrosymmetric spatial group *Fdd*2. The central C atom shows an angle slightly wider [116.3 (4)°] than that typical of sp^3-hybridation, probably due to the presence of the S atoms; the value is similar to that previously reported for bis[(pyridin-4-yl)sulfanyl]methane (Carballo *et al.*, 2007, 2008*a*,*b*, 2009; Lago *et al.*, 2013, 2014). The S—CH_2—S plane forms an angle of 78.66 (8)° with the planes of the pyridine rings, which are placed in opposite directions relative to the central CH_2 unit; this arrangement is also observed in the reported derivatives where bis[(pyridin-4-yl)sulfanyl]methane behaves as a ligand (Carballo *et al.*, 2007, 2008*a*,*b*, 2009; Lago *et al.*, 2013, 2014). This arrangement is the origin of the conformational chirality shown by this compound (Fig. 4). In our case, this disposition is also influenced by the presence of a hydrogen bond involving one chloride anion and the proton bonded to atom C4 of the ring. This conformation is reinforced by a chalcogen bond established between the Cl and S atoms [S···Cl = 3.373 (4) Å and C—S···Cl = 156.94 (5)°], which is significantly shorter than the van der Waals radii radius sum (3.55 Å; Bondi, 1964). Although the S atom can present two σ-holes, in this case, only one interaction is observed with the chloride anion.

As mentioned before, the formation of the cation in **2** is an unusual reaction. Although similar substitution reactions have been reported for some secondary aliphatic (Souquet *et al.*, 1993), alicyclic (Matsumoto *et al.*, 1984) or heteroaromatic amines (Juliá *et al.*, 1982; Zhao *et al.*, 2011), the process usually takes place under special conditions, such as very high pressures or in highly polar solvent mixtures. Futhermore, it should be noted that the formation of the neutral equivalent bis[(pyridin-4-yl)sulfanyl]methane from pyridine-4-thiol in the presence of CH_2Cl_2 has been described previously in basic conditions, *i.e.* in an alcoholic solution with an excess of NaOH, the reaction taking several days to complete (Amoedo-Portela *et al.*, 2005). In our case, the mechanism is different, as shown in the reaction pathway displayed in Fig. 5. Taking into account our previous studies, we have detected that the first step that implies the substitution of the chloride is the rate-determining step, and it proceeds *via* an S_{N^2} mechanism. This process leads to a reactive chloromethyl intermediate $–CH_2Cl^+$ which evolves quickly to the final product where both Cl atoms have been displaced (Sánchez-Roa *et al.*, 2018). Hence, in this case, the IC_6F_4I role would be as a catalyst.

4. Conclusions

The substituted pyridine pyridine-4-thiol can behave as a HaB acceptor, having a preference for the S atom as the acceptor. In the cocrystal obtained, the concomitant presence of a HaB and a hydrogen bond contributes to the stabilization of the zwitterionic form of pyridine-4-thiol. This arrangement has an effect on the reactivity and the activation of CH_2Cl_2 is promoted to give the bis[(4-pyridin-1-ium-4-yl)sulfanyl]methane dication, where two sulfide–pyridinium units are bonded to a $–CH_2$ group. This moiety could only come from the activation of the dichloromethane present as a solvent. Interestingly, there are not many examples of this type of activity and the current study opens up the possibility of developing processes for the transformation of chorinated hydrocarbons.

Acknowledgements

The authors would like to acknowledge the support of Alcalá University, Spain, and the Madrid Regional Government.

Funding information

Funding for this research was provided by: Universidad de Alcala (grant No. PIUAH21/CC-028); Madrid Regional Government (grant No. EPUINV/2020/001).

References

Aakeröy, C. B., Baldrighi, M., Desper, J., Metrangolo, P. & Resnati, G. (2013). *Chem. Eur. J.* **19**, 16240–16247.
Amoedo-Portela, A., Carballo, R., Casas, J. S., García-Martínez, E., Lago-Blanco, A. B., Sánchez-González, A., Sordo, J. & Vázquez-López, E. M. (2005). *Z. Anorg. Allg. Chem.* **631**, 2241–2246.
Arman, H. D., Kaulgud, T. & Tiekink, E. R. T. (2010). *Acta Cryst.* E**66**, o2683.
Bamberger, J., Ostler, F. & Mancheño, O. G. (2019). *ChemCatChem*, **11**, 5198–5211.
Blessing, R. H. (1995). *Acta Cryst.* A**51**, 33–38.
Bondi, A. (1964). *J. Phys. Chem.* **68**, 441–451.
Bozopoulos, A. P. & Rentzeperis, P. J. (1986). *Acta Cryst.* C**42**, 1014–1016.
Brammer, L., Bruton, E. A. & Sherwood, P. (2001). *Cryst. Growth Des.* **1**, 277–290.
Bulfield, D. & Huber, S. M. (2016). *Chem. Eur. J.* **22**, 14434–14450.
Carballo, R., Covelo, B., Fernández-Hermida, N., García-Martinez, E., Lago, A. B. & Vázquez-López, E. M. (2008*a*). *Cryst. Growth Des.* **8**, 995–1004.
Carballo, R., Covelo, B., Fernández-Hermida, N., García-Martínez, E., Lago, A. B. & Vázquez-López, E. M. (2008*b*). *J. Mol. Struct.* **892**, 427–432.
Carballo, R., Covelo, B., Fernández-Hermida, N., Lago, A. B. & Vázquez-López, E. M. (2009). *CrystEngComm*, **11**, 817.
Carballo, R., Covelo, B., García-Martínez, E., Lago, A. B. & Vázquez-López, E. M. (2007). *Z. Anorg. Allg. Chem.* **633**, 780–782.
Cavallo, G., Metrangolo, P., Milani, R., Pilati, T., Priimagi, A., Resnati, G. & Terraneo, G. (2016). *Chem. Rev.* **116**, 2478–2601.
Ding, X., Tuikka, M. & Haukka, M. (2020). *Crystals*, **10**, 165.
Dortéz, S., Fernández-Palacio, F., Damián, J., Gaiteiro, C., Ramos, J., Gómez-Sal, P. & Mosquera, M. E. G. (2020). *CrystEngComm*, **22**, 870–877.
Duisenberg, A. J. M., Kroon-Batenburg, L. M. J. & Schreurs, A. M. M. (2003). *J. Appl. Cryst.* **36**, 220–229.
Farrugia, L. J. (2012). *J. Appl. Cryst.* **45**, 849–854.
Groom, C. R., Bruno, I. J., Lightfoot, M. P. & Ward, S. C. (2016). *Acta Cryst.* B**72**, 171–179.
Hirschberg, M. E., Barthen, P., Frohn, H., Bläser, D., Tobey, B. & Jansen, G. (2014). *J. Fluor. Chem.* **163**, 28–33.
Jónsson, H. F., Sethio, D., Wolf, J., Huber, S. M., Fiksdahl, A. & Erdelyi, M. (2022). *ACS Catal.* **12**, 7210–7220.
Juliá, S., Sala, P., Del Mazo, J., Sancho, M., Ochoa, C., Elguero, J., Fayet, J. & Vertut, M. (1982). *J. Heterocycl. Chem.* **19**, 1141–1145.
Lago, A. B., Carballo, R., Rodríguez-Hermida, S. & Vázquez-López, E. M. (2013). *CrystEngComm*, **15**, 1563.
Lago, A. B., Carballo, R., Rodríguez–Hermida, S. & Vázquez–López, E. M. (2014). *Cryst. Growth Des.* **14**, 3096.

Matsumoto, K., Hashimoto, S., Ikemi, Y. & Otani, S. (1984). *Heterocycles*, **22**, 1417–1420.
Mosquera, M. E. G., Egido, I., Hortelano, C., López-López, M. & Gómez-Sal, P. (2017). *Faraday Discuss.* **203**, 257–283.
Mosquera, M. E. G., Gomez-Sal, P., Díaz, I., Aguirre, L. M., Ienco, A., Manca, G. & Mealli, C. (2016). *Inorg. Chem.* **55**, 283–291.
Nonius (2004). *COLLECT*. Nonius BV, Delft, The Netherlands.
Parsons, S., Flack, H. D. & Wagner, T. (2013). *Acta Cryst.* B**69**, 249–259.
Politzer, P., Lane, P., Concha, M. C., Ma, Y. & Murray, J. S. (2007). *J. Mol. Model.* **13**, 305–311.
Postnikov, P. S., Guselnikova, O. A., Yusubov, M. S., Yoshimura, A., Nemykin, V. N. & Zhdankin, V. V. (2015). *J. Org. Chem.* **80**, 5783–5788.
Sánchez-Roa, D., Santiago, T. G., Fernández-Millán, M., Cuenca, T., Palma, P., Cámpora, J. & Mosquera, M. E. G. (2018). *Chem. Commun.* **54**, 12586–12589.
Sheldrick, G. M. (2008). *Acta Cryst.* A**64**, 112–122.
Sheldrick, G. M. (2015*a*). *Acta Cryst.* A**71**, 3–8.
Sheldrick, G. M. (2015*b*). *Acta Cryst.* C**71**, 3–8.
Soldatova, N. S., Postnikov, P. S., Suslonov, V. V., Kissler, T. Yu., Ivanov, D. M., Yusubov, M. S., Galmés, B., Frontera, A. & Kukushkin, V. Yu. (2020). *Org. Chem. Front.* **7**, 2230–2242.
Souquet, F., Martens, T. & Fleury, M. B. (1993). *Synth. Commun.* **23**, 817–828.
Vidal, F., Dávila, M. A., Torcuato, A. S., Gómez-Sal, P. & Mosquera, M. E. G. (2013). *Dalton Trans.* **42**, 7074–7084.
Zhao, X., Wu, T., Bu, X. & Feng, P. (2011). *Dalton Trans.* **40**, 8072–8074.
Zuluaga, A. R., Brock, A. J., Pfrunder, M. C., Phonsri, W., Murray, K. S., Harding, P., Micallef, A. S., Postnikov, P. S., Guselnikova, O. A., Yusubov, M. S., Yoshimura, A., Nemykin, V. N. & Zhdankin, V. V. (2015). *J. Org. Chem.* **80**, 5783.

supporting information

Acta Cryst. (2023). C**79**, 112-117 [https://doi.org/10.1107/S205322962300205X]

Pyridine-4-thiol as halogen-bond (HaB) acceptor: influence of the noncovalent interaction in its reactivity

Marta E. G. Mosquera, Silvia Dortez, Francisco Fernández-Palacio and Pilar Gómez-Sal

Computing details

For both structures, data collection: *COLLECT* (Nonius, 2004); cell refinement: *DIRAX/LSQ* (Duisenberg *et al.*, 2003); data reduction: *EVALCCD* (Duisenberg *et al.*, 2003). Program(s) used to solve structure: SHELXT2018 (Sheldrick, 2015*a*) for (1); *SHELXS2013* (Sheldrick, 2008) for (2). Program(s) used to refine structure: *SHELXL2016* (Sheldrick, 2015*b*) for (1); *SHELXL2014* (Sheldrick, 2015*b*) for (2). For both structures, molecular graphics: *ORTEP-3 for Windows* (Farrugia, 2012); software used to prepare material for publication: *WinGX* (Farrugia, 2012).

1,2,4,5-Tetrafluoro-3,6-diiodobenzene bis(pyridin-1-ium-4-ylsulfanide) (1)

Crystal data

$C_6F_4I_2·2C_5H_5NS$
M_r = 624.18
Monoclinic, $P2_1/c$
Hall symbol: -P 2ybc
a = 16.288 (8) Å
b = 5.790 (4) Å
c = 10.546 (9) Å
β = 104.77 (3)°
V = 961.7 (12) Å^3
Z = 2
$F(000)$ = 588
D_x = 2.155 Mg m^{-3}
Mo $K\alpha$ radiation, λ = 0.71073 Å
Cell parameters from 215 reflections
θ = 3.2–16.1°
μ = 3.53 mm^{-1}
T = 200 K
Prism, pale yellow
0.21 × 0.18 × 0.15 mm

Data collection

Nonius KappaCCD diffractometer
Radiation source: Enraf Nonius FR590
Graphite monochromator
Detector resolution: 9 pixels mm^{-1}
CCD rotation images, thick slices scans
Absorption correction: multi-scan (Blessing, 1995)
T_{min} = 0.371, T_{max} = 0.426
3983 measured reflections
2181 independent reflections
1458 reflections with $I > 2\sigma(I)$
R_{int} = 0.040
θ_{max} = 27.5°, θ_{min} = 3.8°
h = 0→21
k = −7→7
l = −13→13

Refinement

Refinement on F^2
Least-squares matrix: full
$R[F^2 > 2\sigma(F^2)]$ = 0.032
$wR(F^2)$ = 0.069
S = 0.93
2181 reflections
122 parameters
0 restraints
0 constraints
Hydrogen site location: mixed
H atoms treated by a mixture of independent and constrained refinement
$w = 1/[\sigma^2(F_o^2) + (0.0226P)^2]$ where $P = (F_o^2 + 2F_c^2)/3$

$(\Delta/\sigma)_{max}$ = 0.001
$\Delta\rho_{max}$ = 0.99 e Å^{-3}
$\Delta\rho_{min}$ = −1.09 e Å^{-3}

Special details

Geometry. All esds (except the esd in the dihedral angle between two l.s. planes) are estimated using the full covariance matrix. The cell esds are taken into account individually in the estimation of esds in distances, angles and torsion angles; correlations between esds in cell parameters are only used when they are defined by crystal symmetry. An approximate (isotropic) treatment of cell esds is used for estimating esds involving l.s. planes.

Refinement. Data collection was performed at 200 (2) K, with the crystals covered with perfluorinated ether oil. Single crystals were mounted on a Bruker-Nonius Kappa CCD single crystal diffractometer equipped with a graphite-monochromated Mo-Kα radiation (λ = 0.71073 Å). Multiscan absorption correction procedures were applied to the data (Blessing, 1995). The structure was solved using the WINGX package, (Farrugia, 2012) by direct methods (SHELXS-2013) and refined using full-matrix least-squares against F^2 (SHELXL-2016).(Sheldrick, 2015) All non-hydrogen atoms were anisotropically refined.
Full-matrix least-squares refinements were carried out by minimizing w(Fo^2 - Fc^2)^2 with the SHELXL2014 weighting scheme and stopped at shift/err < 0.001. The final residual electron density maps showed no remarkable features. Crystallographic data for the structure reported in this paper have been deposited with the Cambridge Crystallographic Data Centre as supplementary publication no. CCDC-2222767 [**1**] and 2222766 [**2**].

Fractional atomic coordinates and isotropic or equivalent isotropic displacement parameters (Å^2)

	x	*y*	*z*	U_{iso}*/U_{eq}
C1	0.8563 (3)	0.0026 (8)	0.2712 (4)	0.0330 (10)
C2	0.7891 (3)	−0.1543 (8)	0.2540 (5)	0.0350 (11)
H2	0.74811	−0.136116	0.303246	0.042*
C3	0.7815 (3)	−0.3326 (8)	0.1679 (5)	0.0397 (11)
H3	0.735913	−0.439004	0.158066	0.048*
C4	0.9026 (3)	−0.2109 (9)	0.1069 (5)	0.0400 (12)
H4	0.94134	−0.231938	0.054024	0.048*
C5	0.9132 (3)	−0.0325 (9)	0.1917 (4)	0.0387 (11)
H5	0.959431	0.070832	0.198036	0.046*
C6	0.5758 (3)	0.4353 (8)	0.4694 (4)	0.0312 (10)
C7	0.5349 (3)	0.6360 (8)	0.4217 (5)	0.0365 (11)
C8	0.4605 (3)	0.7008 (8)	0.4527 (5)	0.0354 (11)
F1	0.56773 (17)	0.7763 (5)	0.3454 (3)	0.0503 (8)
F2	0.42425 (16)	0.8996 (4)	0.4053 (3)	0.0434 (7)
I1	0.69103 (2)	0.34216 (5)	0.42717 (3)	0.03545 (12)
N1	0.8384 (3)	−0.3580 (7)	0.0967 (4)	0.0380 (9)
S1	0.87081 (7)	0.2220 (2)	0.38297 (12)	0.0365 (3)
H1	0.831 (3)	−0.461 (8)	0.043 (4)	0.032 (14)*

Atomic displacement parameters (Å^2)

	U^{11}	U^{22}	U^{33}	U^{12}	U^{13}	U^{23}
C1	0.032 (2)	0.038 (3)	0.030 (3)	0.008 (2)	0.008 (2)	0.004 (2)
C2	0.035 (2)	0.040 (3)	0.036 (3)	−0.001 (2)	0.018 (2)	0.000 (2)
C3	0.045 (3)	0.037 (3)	0.041 (3)	0.000 (2)	0.018 (2)	0.006 (2)
C4	0.032 (2)	0.056 (3)	0.036 (3)	0.007 (2)	0.014 (2)	−0.004 (2)
C5	0.033 (2)	0.050 (3)	0.035 (3)	−0.001 (2)	0.013 (2)	−0.001 (2)
C6	0.027 (2)	0.034 (3)	0.034 (3)	0.0017 (19)	0.009 (2)	−0.004 (2)

C7	0.033 (2)	0.041 (3)	0.038 (3)	−0.005 (2)	0.015 (2)	0.003 (2)
C8	0.035 (2)	0.030 (3)	0.041 (3)	0.004 (2)	0.010 (2)	0.002 (2)
F1	0.0504 (17)	0.0465 (17)	0.064 (2)	0.0074 (13)	0.0331 (16)	0.0169 (15)
F2	0.0435 (15)	0.0363 (16)	0.0520 (18)	0.0113 (12)	0.0151 (14)	0.0109 (13)
I1	0.03240 (17)	0.03685 (19)	0.0390 (2)	0.00084 (13)	0.01266 (13)	−0.00130 (15)
N1	0.046 (2)	0.037 (2)	0.032 (2)	0.001 (2)	0.0113 (19)	−0.003 (2)
S1	0.0339 (6)	0.0380 (7)	0.0417 (7)	−0.0022 (5)	0.0170 (6)	−0.0026 (5)

Geometric parameters (Å, º)

C1—C2	1.398 (6)	C6—C7	1.370 (6)
C1—C5	1.415 (5)	C6—C8^{i}	1.376 (6)
C1—S1	1.708 (5)	C6—I1	2.107 (4)
C2—C3	1.360 (6)	C7—F1	1.346 (5)
C3—N1	1.341 (6)	C7—C8	1.385 (6)
C4—N1	1.332 (6)	C8—F2	1.332 (5)
C4—C5	1.348 (6)		
C2—C1—C5	116.1 (4)	C8^{i}—C6—I1	121.4 (3)
C2—C1—S1	122.6 (3)	F1—C7—C6	120.1 (4)
C5—C1—S1	121.3 (3)	F1—C7—C8	118.8 (4)
C3—C2—C1	121.0 (4)	C6—C7—C8	121.1 (4)
N1—C3—C2	120.0 (4)	F2—C8—C6^{i}	120.1 (4)
N1—C4—C5	120.6 (4)	F2—C8—C7	118.5 (4)
C4—C5—C1	120.7 (4)	C6^{i}—C8—C7	121.4 (4)
C7—C6—C8^{i}	117.6 (4)	C4—N1—C3	121.7 (4)
C7—C6—I1	121.0 (3)		

Symmetry code: (i) −*x*+1, −*y*+1, −*z*+1.

4,4′-[Methanediyldi(sulfanediyl)]dipyridinium dichloride (2)

Crystal data

$C_{11}H_{12}N_2S_2^{2+}\cdot 2Cl^-$
M_r = 307.25
Orthorhombic, *F*2*dd*
Hall symbol: F -2d 2
a = 8.0815 (4) Å
b = 17.2161 (5) Å
c = 18.9254 (12) Å
V = 2633.1 (2) Å^3
Z = 8
F(000) = 1264
D_x = 1.55 Mg m^{-3}
Mo *Kα* radiation, *λ* = 0.71073 Å
Cell parameters from 211 reflections
θ = 3.4–16.4°
μ = 0.79 mm^{-1}
T = 200 K
Prism, brown
0.4 × 0.3 × 0.25 mm

Data collection

Nonius KappaCCD diffractometer
Radiation source: Enraf Nonius FR590
Horizonally mounted graphite crystal monochromator
Detector resolution: 9 pixels mm^{-1}
CCD rotation images, thick slices scans
4579 measured reflections
1386 independent reflections
1177 reflections with $I > 2\sigma(I)$
R_{int} = 0.069
θ_{max} = 27.5°, θ_{min} = 3.2°
h = −10→9
k = −22→22
l = −22→24

Refinement

Refinement on F^2
Least-squares matrix: full
$R[F^2 > 2\sigma(F^2)] = 0.041$
$wR(F^2) = 0.101$
$S = 1.10$
1386 reflections
84 parameters
1 restraint
0 constraints
Hydrogen site location: mixed
H atoms treated by a mixture of independent and constrained refinement
$w = 1/[\sigma^2(F_o^2) + (0.0356P)^2 + 12.059P]$ where $P = (F_o^2 + 2F_c^2)/3$
$(\Delta/\sigma)_{max} = 0.001$
$\Delta\rho_{max} = 0.35$ e Å^{-3}
$\Delta\rho_{min} = -0.30$ e Å^{-3}
Absolute structure: Flack *x* determined using 445 quotients [(I+)-(I-)]/[(I+)+(I-)] (Parsons *et al.*, 2013)
Absolute structure parameter: −0.01 (11)

Special details

Geometry. All esds (except the esd in the dihedral angle between two l.s. planes) are estimated using the full covariance matrix. The cell esds are taken into account individually in the estimation of esds in distances, angles and torsion angles; correlations between esds in cell parameters are only used when they are defined by crystal symmetry. An approximate (isotropic) treatment of cell esds is used for estimating esds involving l.s. planes.

Refinement. Data collection was performed at 200 (2) K, with the crystals covered with perfluorinated ether oil. Single crystals were mounted on a Bruker-Nonius Kappa CCD single crystal diffractometer equipped with a graphite-monochromated Mo-Kα radiation (λ = 0.71073 Å). Multiscan absorption correction procedures were applied to the data (Blessing, 1995). The structure was solved using the WINGX package, (Farrugia, 2012) by direct methods (SHELXS-2013) and refined using full-matrix least-squares against F^2 (SHELXL-2016).(Sheldrick, 2015) All non-hydrogen atoms were anisotropically refined.
Full-matrix least-squares refinements were carried out by minimizing w(Fo^2 - Fc^2)^2 with the SHELXL2014 weighting scheme and stopped at shift/err < 0.001. The final residual electron density maps showed no remarkable features. Crystallographic data for the structure reported in this paper have been deposited with the Cambridge Crystallographic Data Centre as supplementary publication no. CCDC-2222767 [**1**] and 2222766 [**2**].

Fractional atomic coordinates and isotropic or equivalent isotropic displacement parameters (Å^2)

	x	*y*	*z*	U_{iso}*/U_{eq}
C10	1.9499 (10)	1.25	0.75	0.0248 (15)
C1	1.6370 (7)	1.0985 (3)	0.9457 (3)	0.0323 (13)
H1	1.5814	1.0546	0.9619	0.039*
C3	1.7388 (8)	1.2237 (3)	0.9678 (3)	0.0300 (13)
H3	1.7541	1.2646	0.9992	0.036*
C4	1.7957 (7)	1.2300 (3)	0.8997 (3)	0.0260 (12)
H4	1.8489	1.275	0.8847	0.031*
C5	1.7723 (7)	1.1679 (3)	0.8535 (2)	0.0212 (10)
C6	1.6931 (7)	1.1010 (3)	0.8784 (3)	0.0268 (12)
H6	1.679	1.0584	0.8487	0.032*
N1	1.6613 (6)	1.1590 (3)	0.9894 (2)	0.0283 (11)
S1	1.83235 (15)	1.16275 (8)	0.76516 (6)	0.0270 (4)
Cl	1.25853 (17)	1.16469 (7)	0.86975 (6)	0.0280 (3)
H10A	2.014 (9)	1.262 (3)	0.793 (3)	0.04*
H1N	1.627 (9)	1.153 (4)	1.035 (4)	0.05*

Atomic displacement parameters (Å^2)

	U^{11}	U^{22}	U^{33}	U^{12}	U^{13}	U^{23}
C10	0.025 (4)	0.027 (4)	0.023 (3)	0	0	0.010 (3)

C1	0.034 (3)	0.032 (3)	0.031 (3)	−0.006 (2)	0.000 (2)	0.010 (2)
C3	0.043 (4)	0.025 (3)	0.021 (2)	0.006 (3)	0.001 (2)	−0.001 (2)
C4	0.035 (3)	0.019 (3)	0.024 (2)	−0.001 (2)	0.000 (2)	0.0028 (19)
C5	0.021 (2)	0.024 (2)	0.019 (2)	0.000 (2)	0.000 (2)	0.0024 (18)
C6	0.031 (3)	0.022 (2)	0.027 (3)	−0.005 (2)	−0.002 (2)	−0.003 (2)
N1	0.036 (3)	0.032 (3)	0.017 (2)	0.005 (2)	0.0056 (19)	0.0041 (18)
S1	0.0396 (8)	0.0235 (6)	0.0179 (6)	−0.0028 (6)	0.0029 (6)	0.0006 (5)
Cl	0.0376 (7)	0.0253 (6)	0.0210 (6)	−0.0034 (5)	0.0058 (6)	−0.0024 (5)

Geometric parameters (Å, º)

C10—S1	1.800 (4)	C3—C4	1.371 (7)
C10—S1^{i}	1.800 (4)	C4—C5	1.394 (7)
C1—N1	1.344 (7)	C5—C6	1.400 (7)
C1—C6	1.354 (7)	C5—S1	1.743 (5)
C3—N1	1.342 (7)		
S1—C10—S1^{i}	116.3 (4)	C4—C5—S1	127.1 (4)
N1—C1—C6	120.4 (5)	C6—C5—S1	114.0 (4)
N1—C3—C4	120.6 (5)	C1—C6—C5	119.7 (5)
C3—C4—C5	118.9 (5)	C3—N1—C1	121.6 (5)
C4—C5—C6	118.8 (4)	C5—S1—C10	104.89 (19)

Symmetry code: (i) x, $-y+5/2$, $-z+3/2$.